INL/CON-07-12487
PREPRINT

Accuracy and Efficiency of a Coupled Neutronics and Thermal Hydraulics Model

NURETH-12

Michael A. Pope
Vincent A. Mousseau

September 2007

The INL is a
U.S. Department of Energy
National Laboratory
operated by
Battelle Energy Alliance

Idaho National Laboratory

Accuracy and Efficiency of a Coupled Neutronics and Thermal Hydraulics Model

Michael A. Pope and Vincent A. Mousseau*
Idaho National Laboratory
PO Box 1625, Idaho Falls, Idaho, 83415-3840
michael.pope@inl.gov; vincent.mousseau@inl.gov*

ABSTRACT

The accuracy requirements for modern nuclear reactor simulation are steadily increasing due to the cost and regulation of relevant experimental facilities. Because of the increase in the cost of experiments and the decrease in the cost of simulation, simulation will play a much larger role in the design and licensing of new nuclear reactors. Fortunately, as the work load of simulation increases, there are better physics models, new numerical techniques, and more powerful computer hardware that will enable modern simulation codes to handle the larger workload. This manuscript will discuss a numerical method where the six equations of two-phase flow, the solid conduction equations, and the two equations that describe neutron diffusion and delayed neutron precursor concentration are solved together in a tightly coupled, nonlinear fashion for a simplified model of a nuclear reactor core. This approach has two important advantages. The first advantage is a higher level of accuracy. Because the equations are solved together in a single nonlinear system, the solution is more accurate than the traditional "operator split" approach where the two-phase flow equations are solved first, the heat conduction is solved second and the neutron diffusion is solved third, limiting the temporal accuracy to 1st order because the nonlinear coupling between the physics is handled explicitly. The second advantage of the method described in this manuscript is that the time step control in the fully implicit system can be based on the timescale of the solution rather than a stability-based time step restriction like the material Courant. Results are presented from a simulated control rod movement and a rod ejection that address temporal accuracy for the fully coupled solution and demonstrate how the fastest timescale of the problem can change between the state variables of neutronics, heat conduction and two-phase flow during the course of a transient.

KEYWORDS
modeling, simulation, JFNK, fully-implicit, coupled

1. INTRODUCTION

The current generation of tools used in the United States for thermal hydraulic simulation of nuclear power plants, such as RELAP5 [1] and TRAC [2], were written in the 1970's. Because of constraints on computer speed and memory at the time of their inception, sacrifices were made in terms of physical models and numerical methods. For example, different types of physics (neutron diffusion, heat conduction and two-phase fluid flow) were handled separately by what often originated as stand-alone simulation tools. The results of these separate tools were then

loosely coupled by the high-level software package to represent the transient. This type of "operator splitting" remains standard practice among the current state-of-the-art nuclear power plant system safety analysis software. Regardless of the order in which the various tools are used within the software, the values of some of the variables at new time are calculated based on variables and/or closure relations available only at old time. This traditional approach nearly always limits the temporal accuracy of the entire algorithm to 1st order in a transient simulation, regardless of the accuracy of the constituent solution algorithms for each type of physics [3] and can lead to oscillations which may prevent convergence in a steady state problem [4] (Note: 2nd order in time operator split algorithms are possible).

Since the 1970's, exponential increases have been realized in computing speed and memory size accompanied by ever-decreasing costs. With today's machines, it is possible to take advantage of new numerical algorithms which allow for fully implicit solution of large non-linear systems of partial differential equations (PDE's) with 2nd order accuracy in time. Rather than splitting the different types of physics, they can remain tightly coupled and all variables and constitutive relations can be solved for simultaneously at new time.

This work involves the simulation of a simplified nuclear reactor core wherein nine nonlinearly coupled PDE's are discretized and solved simultaneously using the 2nd order in time physics-based preconditioned Jacobian Free Newton-Krylov (JFNK) method [5,6,7]. The equations solved are the six equations of 1-D two phase flow, a single 2-D heat conduction equation and 2-D neutron diffusion and precursor concentration equations. A similar reactor model was used in previous work in order to demonstrate the advantages of JFNK methods over operator splitting [3].

2. OBJECTIVES

The work presented in this manuscript represents several key changes to the reactor model used in previous work described in [3]. Firstly, more realistic neutronic parameters (cross-sections and delayed neutron fraction) were added in order to portray more realistic timescales for the simulations. Secondly, a basic model was added to simulate decay heat generation after reactor shutdown. Finally, a control rod model was added.

In this work, the control rod was manipulated to create three different types of transients. The first was a slow transient in which the rod was moved with a prescribed position versus time. This transient was used to demonstrate that the simulation was 2nd order accurate in time with the control rod model. The other two types of transients simulated were rod ejection accidents (REA's). The first type of REA was an instantaneous ejection used to demonstrate the various timescales of state variables in the problem and the advantages of the time step control of JFNK methods. Three more REA transients were simulated with rod ejection times of 0.01, 0.05 and 0.1 seconds. The effects of the three ejection speeds are compared with the results of the instantaneous rod ejection.

3. DESCRIPTION OF MODEL

3.1. PDE's and Closure Models

The nine PDE's solved in this simulation are described briefly in this section along with some mention of closure models. For a more complete description of the equations, closure models and the solution method, see [4,6,7].

The conservation of mass in the vapor phase is given by

$$\frac{\partial \alpha_g \rho_g}{\partial t} + \frac{\partial \alpha_g \rho_g v_g}{\partial x} = \Gamma_g \tag{1}$$

where α is the volume fraction, ρ is mass density, v is velocity, t is time, x is position, Γ_g is interphase mass transfer from liquid to vapor and the subscript g refers to the vapor phase. The conservation of mass in the liquid phase is given by

$$\frac{\partial \alpha_f \rho_f}{\partial t} + \frac{\partial \alpha_f \rho_f v_f}{\partial x} = -\Gamma_g \tag{2}$$

where the subscript f refers to the liquid phase.

The conservation of momentum for the vapor phase is given by

$$\alpha_g \rho_g \frac{\partial v_g}{\partial t} + \alpha_g \rho_g v_g \frac{\partial v_g}{\partial x} + \alpha_g \frac{\partial P}{\partial x} = -F_{wg} a_{wg} \left(\alpha_g \rho_g\right)^2 |v_g| v_g \\ - a_i FI |v_g - v_f| (v_g - v_f) - \Gamma_g (v_i - v_g) \tag{3}$$

where P is pressure, a_{wg} is the wall surface area in contact with vapor, F_{wg} is the wall friction coefficient corresponding to the vapor phase, a_i is the interfacial area between phases, and FI is the interfacial friction coefficient. The conservation of momentum for the liquid phase is given by

$$\alpha_f \rho_f \frac{\partial v_f}{\partial t} + \alpha_f \rho_f v_f \frac{\partial v_f}{\partial x} + \alpha_f \frac{\partial P}{\partial x} = -F_{wf} a_{wf} \left(\alpha_f \rho_f\right)^2 |v_f| v_f \\ + a_i FI |v_g - v_f| (v_g - v_f) - \Gamma_g (v_i - v_f) \tag{4}$$

where a_{wf} is the wall surface area in contact with liquid and F_{wg} is the wall friction coefficient corresponding to the liquid phase. The interfacial velocity term v_i in Equations 3 and 4 is given by the following simplified model

$$v_i = \frac{1}{2}\left(v_g + v_f\right) \tag{5}$$

The equation for conservation of energy in the vapor phase is as follows

$$\frac{\partial \, \alpha_g \, \rho_g \, U_g}{\partial t} + \frac{\partial \, \alpha_g \, \rho_g \, U_g \, v_g}{\partial x} + P \frac{\partial \, \alpha_g}{\partial t} + P \frac{\partial \alpha_g v_g}{\partial x} =$$
$$H_{wg} \, a_{wg} \left(T_w - T_g\right) + H_{fg} \, a_i \left(T_f - T_g\right) + H_{ig} \, a_i \left(T_s - T_g\right) + \Gamma_g \, h_g^*$$
(6)

where U is specific internal energy, H_{wg} is the wall heat transfer coefficient corresponding to heat transfer from the wall to the vapor, H_{fg} is the heat transfer coefficient between liquid and vapor, H_{ig} is the heat transfer coefficient between the vapor and the interface, T_w is the temperature of the solid fuel, T_g and T_f are vapor and liquid temperatures, respectively, and T_s is the fluid saturation temperature. Similarly, the conservation of energy in liquid phase is given by

$$\frac{\partial \, \alpha_f \, \rho_f \, U_f}{\partial t} + \frac{\partial \, \alpha_f \, \rho_f \, U_f \, v_f}{\partial x} + P \frac{\partial \, \alpha_f}{\partial t} + P \frac{\partial \alpha_f v_f}{\partial x} =$$
$$H_{wf} \, a_{wf} \left(T_w - T_f\right) - H_{fg} \, a_i \left(T_f - T_g\right) + H_{if} \, a_i \left(T_s - T_f\right) - \Gamma_g \, h_f^*$$
(7)

where H_{if} is the heat transfer coefficient between the phase interface and the liquid.

The liquid and vapor mass transfer enthalpies found in Equations 6 and 7 are given in terms of the liquid and vapor enthalpies, h_f and h_g, and the liquid and vapor saturation enthalpies, h_{fs} and h_{gs}, by

$$h_g^* = \begin{cases} h_{gs} & if \quad \Gamma_g > 0 \\ h_g & otherwise \end{cases}$$
(8)

$$h_f^* = \begin{cases} h_f & if \quad \Gamma_g > 0 \\ h_{fs} & otherwise \end{cases}$$
(9)

Conservation of energy in the fuel is given by the following equation

$$\frac{\partial \, e_w}{\partial t} - \frac{\partial}{\partial x} K \, \frac{\partial T_w}{\partial x} - \frac{\partial}{\partial y} K \, \frac{\partial T_w}{\partial y} = \Sigma_f e_f \phi - \left\{ H_{wg} \, a_{wg} \left(T_w - T_g\right) + H_{wf} \, a_{wf} \left(T_w - T_f\right) \right\}$$
(10)

where K is the thermal conductivity, Σ_f is the thermal neutron fission cross-section, e_f is the energy released per fission, ϕ is the thermal neutron flux and e_w is the internal energy in the fuel. It should be noted that only the components of the fuel temperature array (T_w) in contact with the fluid are used in the convection heat transfer (terms in curly brackets in Equation 10). The tight coupling between heat conduction in the solid and neutron diffusion is revealed by the presence of the fission energy as the internal heat source in the solid, given by the $\Sigma_f e_f \phi$ term in Equation 10. The conservation of neutrons is accounted for by the following thermal neutron diffusion equation

$$\frac{1}{v_{th}} \frac{\partial \phi}{\partial t} - \nabla \cdot D \nabla \phi + \Sigma_a \phi - (1 - \beta) \Sigma_f n_f \phi - \lambda C - \tau_{DH} \left[\left| \phi_0 - \phi \right| + \left(\phi_0 - \phi\right) \right]^2 = 0$$
(11)

where v_{th} is the speed of thermal neutrons (2200 m/s), D is the thermal neutron diffusion coefficient, Σ_a is the thermal neutron absorption cross-section, n_f is the number of neutrons emitted per fission reaction, β is the delayed neutron fraction, λ is the decay constant of the delayed neutron precursors and C is the delayed neutron precursor population. In this model, τ_{DH} determines the timescale with which the decay heat model is activated once the flux ϕ drops below a threshold "floor" in the flux denoted by ϕ_0. The delayed neutron precursors are conserved according to the following equation

$$\frac{dC}{dt} - \beta \Sigma_f n_f \phi + \lambda C = 0 \tag{12}$$

Here, one delayed neutron precursor group is assumed with parameters averaged accordingly. A simple decay heat model was used in this work to account for heat generation from fission products and actinides after reactor shutdown. Though not indicated by the forms of Equations 11 and 12, the neutron absorption and fission cross-sections, Σ_a and Σ_f, and the thermal neutron diffusion coefficient D are modeled as functions of the moderator density ρ_m and the fuel temperature T_w, thus preserving the tight coupling between the neutron diffusion, heat conduction and two-phase fluid flow. The forms of these dependences are given in [3].

3.2. Control Rod Model

As was mentioned above, this work involved the incorporation of a control rod model into the reactor simulation. This was modeled as an additional parasitic capture cross section in the nodes that the control rod is adjacent to. The worth of the rod at a certain axial location x is given by

$$\Sigma_{CR}(x) = \frac{1}{2} \Sigma_{CR}^{\max} \left\{ 1 - \tanh\left[\frac{x - X_{rod}}{\delta_{rod}}\right] \right\} \tag{13}$$

where Σ_{CR} is the control rod worth in a node, Σ_{CR}^{max} is the maximum rod worth, x is the axial location of interest, X_{rod} is the position of the end of the control rod and δ_{rod} is the width of the hyperbolic tangent shape in the worth near the end of the rod making it a smooth function of position. The rod location at a given time t^{n+1} is given by

$$X_{rod}^{n+1} = X_{rod}^{n} + \int_{t^n}^{t^{n+1}} V_{rod}(t) \; dt \tag{14}$$

where X_{rod} is the rod axial location and V_{rod} is the rod velocity. It should be emphasized that the time integration of rod velocity in Equation 14 must be performed accurately if the simulation is to be 2nd order accurate in time (it was done analytically in this study). The rod velocity was governed by the following equation

$$V_{rod}(t) = \frac{1}{2}\left[- \tanh\left[\frac{(t_1 - t)}{\delta t}\right] \right] \tag{15}$$

where t_1 is the time to start insertion and δt is the width of the hyperbolic tangents used to simulate stops and starts of the movements smoothly.

3.3. Solution Algorithm

As mentioned above, the simulation uses the 2nd order in time JFNK method with physics-based preconditioning. As this solution method is documented in [4-6], a discussion which will not be given in detail here. The nine equations (Equations 1, 2, 3, 4, 6, 7, 10, 11 and 12) are discretized to give a non-linear system of equations

$$res(x) = 0 \tag{16}$$

where *res* is a vector comprised of the nine discretized conservation equations and x is a vector containing all of the unknowns (v_g, v_f, α_g, P, U_g, U_f, T_w, ϕ, C). Newton's method is used to produce a sequence of linear problems that are then solved by an iterative Krylov method

$$J^k \delta x^k = -res\left(x^k\right) \tag{17}$$

where k is the Newton iteration index. The physics-based preconditioner uses an operator split solution method in order to accelerate the convergence of the Krylov iterations.

3.4. Time Step Control

In discussion of the time step control scheme used in this work, it is instructive to first consider operator split (or semi-implicit) methods. In order for semi-implicit solutions to be numerically stable, they must respect the material Courant limit. Thus the time step is given by

$$t^{n+1} - t^n = \Delta t^n = \min\left(\frac{\eta_{cfl} \Delta x}{\max\left[v_{g,i}^n, v_{f,i}^n \right]} \right) \tag{18}$$

where Δt^n is the time step, Δx is the size of a spatial node, $v_{g,i}^n$ and $v_{f,i}^n$ are vapor and liquid velocities in each mesh location at time step n and η_{cfl} is defined by the user. Simply put, the material Courant limit dictates that in order to maintain numerical stability, no vapor or liquid may completely pass through a calculational node during a single time step. The value of η_{cfl} is a user-specified fraction of that maximum time step which gives the actual time step to be used in the simulation. This type of time step control is common among operator split, or semi-implicit, codes. The maximum time step that would be dictated by the material Courant limit (before the η_{cfl} is applied) is referred to in this work as the CFL.

The weakness of this type of time step control is that it does not consider the timescales of the state variables in the problem. Therefore, the accuracy of the solution is not used in the determination of time step in operator split algorithms. Time steps dictated by the CFL may be much smaller than those required to capture the timescales of the physics in the problem resulting in excessive computation. Conversely, the time step dictated by the CFL may be much

larger than would be required to resolve physics with faster timescales. Unless a time step convergence study is performed, a priori knowledge of the fastest timescales is required for accurate simulation. This is in contrast to the time step control scheme used in the work presented here.

Because of the fully-implicit nature of the 2nd order in time JFNK method, there is no numerical stability limit and the time step can be determined based on the rate at which state variables change. In other words, the size of each time step required to achieve a desired accuracy can be determined based on the fastest timescale of the solution at that time. The time step used here is called a dynamical time step. The concept of a dynamical time scale is introduced by the following equation

$$\tau_\theta = \frac{1}{\left| \frac{1}{\theta} \frac{\partial \theta}{\partial t} \right|} \tag{19}$$

where τ is the dynamical time scale for a certain time step n and a generic state variable θ. The discrete approximation to Equation 19 is given by

$$\tau^n_{\theta,i,j} = \left(\left| \frac{\theta^n_{i,j} - \theta^{n-1}_{i,j}}{\frac{\Delta t^{n-1}}{2} \left[\theta^n_{i,j} + \theta^{n-1}_{i,j} \right]} \right| \right)^{-1} \tag{20}$$

From this, a time step is defined for each variable by

$$\Delta t^n_\theta = \eta_{dyn} \left[\min \tau^n_{\theta,i,j} \right] \tag{21}$$

where $\Delta t_\theta{}^n$ is the size of time step as dictated by the rate of change of generic variable θ and η_{dyn} is a user-defined fractional change allowable in any state variable from one time step to the next. The minimum value of all the time steps computed from all of the state variables is then used for the next time step.

$$\Delta t^n = \min \left(\Delta t^n_{v_g}, \Delta t^n_{v_f}, \Delta t^n_{\alpha_g}, \Delta t^n_P, \Delta t^n_{U_g}, \Delta t^n_{U_f}, \Delta t^n_{T_w}, \Delta t^n_\phi, \Delta t^n_C \right) \tag{22}$$

When the solution changes quickly, small time steps are taken and when the solution is closer to a steady state, very large time steps can be taken. This will be demonstrated in this work using an instantaneous rod ejection accident (REA).

4. RESULTS

4.1. Temporal Accuracy of the Solution

The first calculation to be discussed here is a slow control rod movement. The purpose of this was to demonstrate that the model is 2nd order accurate in time with the control rod motion included. The error for the simulation was computed as the L2 norm of the difference between the computed neutron flux and the neutron flux from a base solution as shown by

$$Error = \sqrt{\sum_{i=1}^{32}\sum_{j=1}^{16}\left(\phi_c\left(i,j\right)-\phi_b\left(i,j\right)\right)^2} \tag{23}$$

where the summations are shown to indicate inclusion of all spatial nodes in two dimensions. Because the system of nine equations cannot be solved analytically, the "base" solution was estimated by using the JFNK method with Δt equal to 0.0625 seconds, which is 10 times smaller than the smallest time step shown in Fig.1. Fig. 1 shows error versus time step. The slope of this line indicates that the simulation is 2nd order accurate in time. This is in contrast to traditional operator split methods, which are 1st order accurate in time at best.
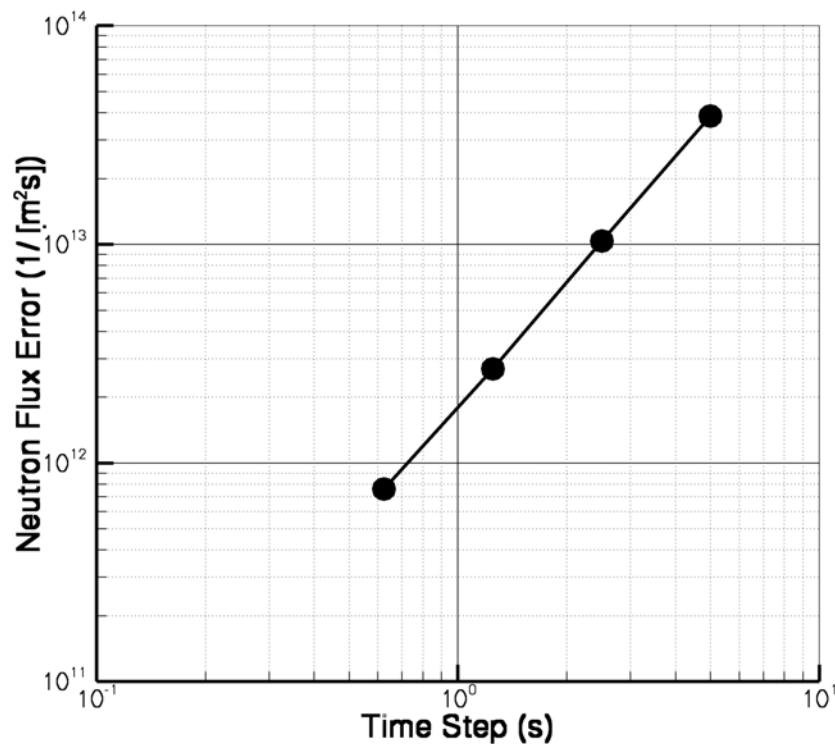

Figure 1. Error versus η_{dyn} for control rod motion using the JFNK solution.

4.2. Timescales of State Variables after an Instantaneous REA

The second transient to be discussed in this Results section is an instantaneous rod ejection. In this transient, the parasitic absorption cross-section from the control rod model is instantaneously removed in all parts of the reactor simultaneously. Fig. 2 shows the normalized power (normalized to the steady state rod-out value) versus time following an instantaneous rod ejection at time zero. Within 1/1000 of a second, the power has peaked at a power approximately eight orders of magnitude greater than the initial value. The Doppler feedback

very quickly reduces the power to a value which remains somewhat steady until approximately 1 second into the transient. During the time from 1 to 100 seconds, the relatively high power continues to increase the temperature of the fuel while heat is conducted out to the cladding and the Doppler feedback and the moderator density coefficient reduce the power further. After approximately 100 seconds, the coolant is able to remove sufficient energy from the fuel to arrest the power decrease. The system then becomes supercritical and power begins to increase again. The result is a return to power excursion occurring at approximately 1000 seconds, after which the power approaches the steady state rod-out value.
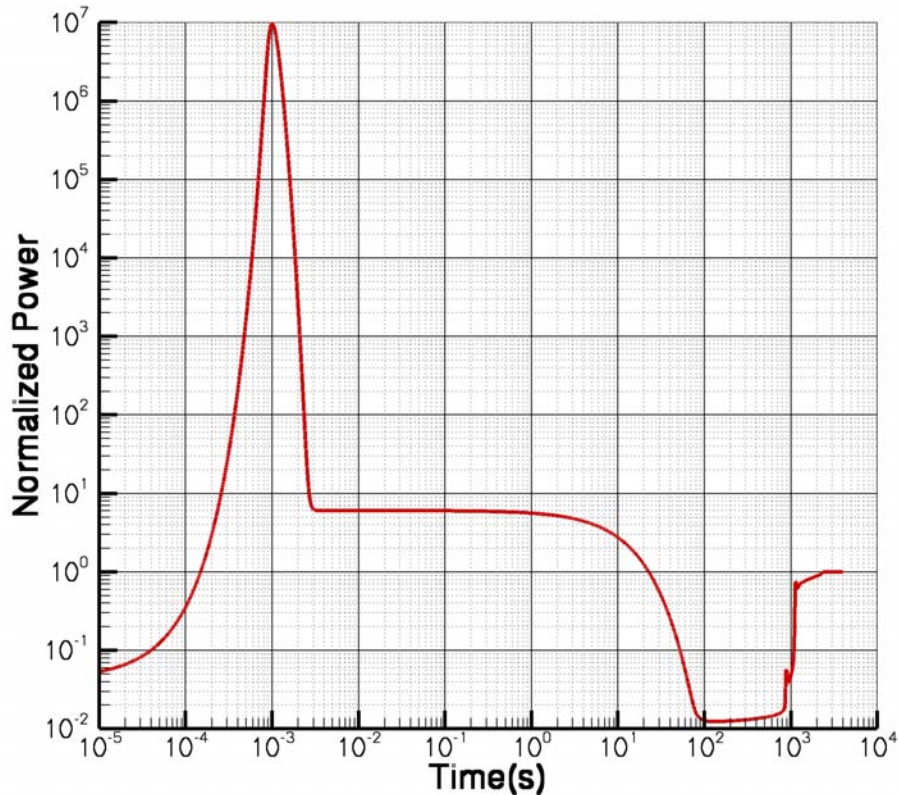

Figure 2. Total neutron flux versus time following instantaneous rod ejection.

It is of interest to examine the timescales of the nine state variables during this simulation. As shown by Equation 21, no state variable is allowed to change by more than a given percent (specified by the parameter η_{dyn}) from one time step to the next. So at any time during the simulation, the fastest-changing variable is setting the time step. Fig. 3 shows the dynamical timescale of each of the nine state variables as calculated using Equation 20. The six blue lines represent the timescales of the two-phase flow variables, the red line is for the heat conduction and the green lines are for neutron flux and precursor concentration. The multicolored line in the figure is the actual time step used, which remains a factor of η_{dyn} below the smallest of the other lines. The color of each section of this line corresponds to what types of state variables are determining the time step at a given time. The dashed line shows the material Courant (CFL) limit.

Initially, the multicolored line giving the actual time step is green, indicating that one of the neutronic state variables (in this case the neutron flux) has the fastest time scale and is therefore setting the simulation time step. This is not surprising given the violence of the power spike observed in Fig. 2.
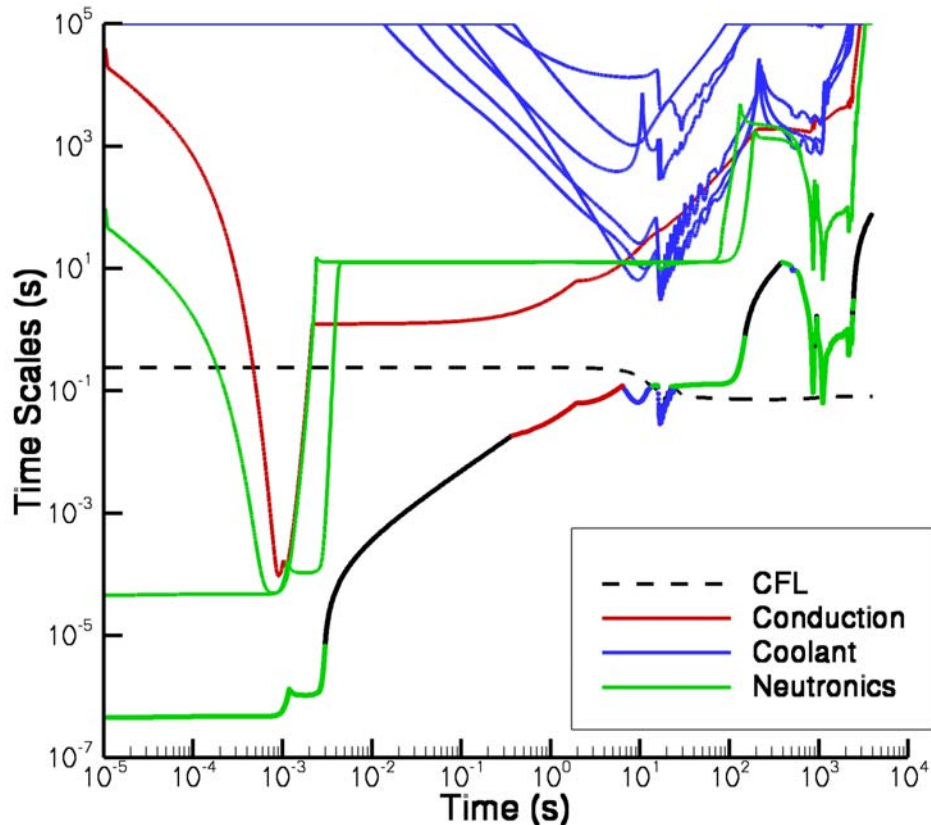

Figure 3. Dynamical timescales of state variables following an instantaneous REA.

At approximately 3×10^{-3} seconds, the multicolored line turns black. The explanation for this has to do with the time step growth rate of 5% which the maximum time step growth from one time step to the next. If the dynamical time-step from Equation (22) increases faster than this user-defined rate, the actual time step grows exponentially limited by the 5% per time step limit. Regions where this is occurring are indicated by the black segments of the multicolored line in Fig. 3.

At approximately 0.3 seconds, the multicolored line in Fig. 3 becomes red. This means that the state variable with the fastest timescale is now the conduction in the solid as the energy deposited in the fuel from fission conducts out to the cladding. At approximately 6 seconds, the multicolored line turns from red to blue indicating that the two-phase flow state variables now set the maximum time step as the coolant has begun to boil aggressively to cool the now hot cladding. At around 20 seconds, the line turns from blue to green as the neutronic timescales are again fastest, and then turns black once again at 130 seconds signifying exponential growth of the time step. The time step continues this exponential growth until around 400 seconds. At this

time, the line turns green again as the neutronics variables change quickly during the return to power transient shown in Fig. 2. Then at 2000 seconds, the line turns black again as the solution approaches steady state.

Though this is a simplified reactor model, the results shown in Fig. 3 indicate that the state variable with the fastest timescale can alternate between neutronics, heat conduction and two-phase fluid flow variables in the course of a transient. The dashed line in Fig. 3 giving the CFL (the maximum time step allowable by the material Courant limit) remains relatively constant, only changing slightly at around 10 seconds from the introduction of faster vapor velocities from boiling. This means that the CFL has not responded at all to the wide variation in timescales of the state variables. The result is that the JFNK method initially takes smaller time steps than the CFL would dictate in order to resolve the very fast physics of the problem solution. After approximately 20 seconds into the transient, the JFNK method takes longer time steps than the CFL would dictate because the state variables are now changing more slowly and the very small time steps are no longer required in order to accurately resolve the physics. By the end of the simulation, the JFNK method is taking time steps roughly 1 minute long, approximately a factor of 1000 larger than the CFL.

One can see how the lack of a stability restriction on time step in JFNK methods makes it conceivable to imagine a single simulation tool capable of handling rather fast transients, such as a scram, and very slow transients, like fuel burnup, in the same computer run.

4.3. Effect of Rod Ejection Speed

The same rod ejection described above as instantaneous is now performed in such a way that it travels out of the core in a specified time. Fig. 4 shows power versus time following each of these simulated rod ejection transients. The ejection times were 0.01, 0.05 and 0.1 seconds represented by the different colored lines and labeled in the legend. The instantaneous rod ejection case is also included in the figure. Similar to Fig. 2, the power is normalized to the steady state rod-out value.

For the three non-instantaneous rod ejections, the power peak is flat on top. Just below the bottom of the control rod the local power increases due to the lower absorption cross section caused by the control rod moving out. This local power rise decreases as Doppler feedback responds. While this power peak moves up the core following the control rod, the total reactor power remains relatively constant. One can also see from Fig. 4 how as the time of rod ejection is decreased, the initial power spike approaches that of the instantaneous rod ejection.
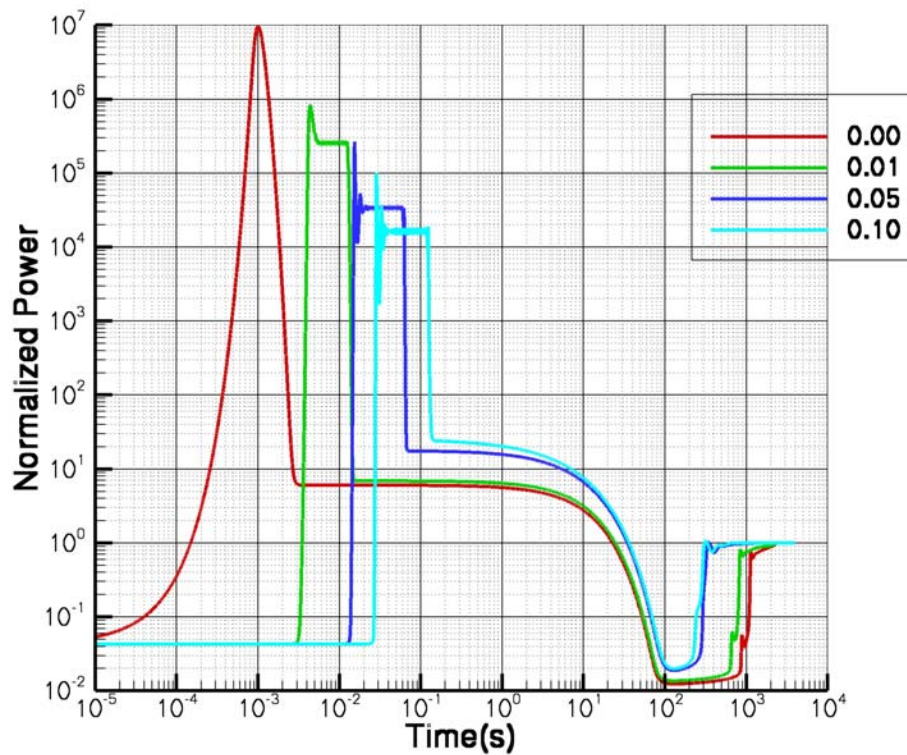
Figure 4. Power versus time for three rod ejection speeds and instantaneous ejection (ejection times given in legend in seconds).

A major difference between the different ejection speeds is the timing of the return to power. For example, this occurs in the 0.01 second ejection case at around 800 second into the transient and at about 300 seconds in the 0.1 second ejection case. While these values are not necessarily representative of the response of a real reactor, this illustrates the need for caution in making assumptions in fast transients. This also demonstrates and the ability of the JFNK solver to capture nonlinear feedback.

5. CONCLUSIONS

In this paper, a simplified slab reactor was modeled using a simulation code which solves coupled neutronics, conduction and two-phase flow equations using the 2nd order in time JFNK algorithm. Because the solution is fully implicit, there is no stability requirement as in the case of operator split methods. This means that the time step control algorithm can be based on resolving the fastest timescales in the problem rather than the material Courant limit. It was demonstrated in this work that under certain circumstances, the variables with the fastest timescales can alternate between neutronics, conduction and two-phase flow during the course of a transient. This means that a code using the JFNK method can take very small time steps while variables change rapidly and then extremely long ones when the problem approaches steady state. A simulated rod ejection with ejection times varying from instantaneous to 1/10 of a second was used to demonstrate how the non-linear feedback can have large effects in transients.

ACKNOWLEDGMENTS

REFERENCES

1. U.S. N.R.C., *RELAP5/MOD3.3 Code Manual Volume I,* NUREG/CR-5535 Edition (December 2001).
2. U.S. N.R.C., *TRAC-M/FORTRAN 90 (Version 3.0) Theory Manual*, NUREG/CR-6724 Edition (April 2001).
3. V.A. Mousseau, "A Fully Implicit, Second Order in Time, Simulation of a Nuclear Reactor Core," *Proceedings of ICONE 14*, Miami, Florida, July 17-20 (2006)
4. V.A. Mousseau, "Implicitly Balanced Solution of the Two-Phase Flow Equations Coupled to Nonlinear Heat Conduction," *Journal of Computational Physics*, **200**, pp.104-132 (2004).
5. D.A. Knoll and D.E. Keyes, "Jacobian-free Newton-Krylov Methods: A Survey of Approaches and Applications", *Journal of Computational Physics*, **193**, pp.357-397 (2004).
6. V.A. Mousseau, "A Fully Implicit Hybrid Solution Method for a Two-Phase Thermal Hydraulic Model," *Journal of Heat Transfer*, **127**, Issue 5, pp.531-539 (2005).
7. V.A. Mousseau, "Accurate Solution of the Nonlinear Partial Differential Equations from Thermal Hydraulics," *Nuclear Technology*, **158**, No. 1, pp.26-35 (2007).